

Limitation of single-repumping schemes for laser cooling of Sr atoms

Naohiro Okamoto,* Takatoshi Aoki, and Yoshio Torii†

Institute of Physics, The University of Tokyo, 3-8-1 Komaba, Meguro-ku, Tokyo 153-8902, Japan

(Dated: June 28, 2024)

We explore the efficacy of two single-repumping schemes, $5s5p^3P_2 - 5p^2^3P_2$ (481 nm) and $5s5p^3P_2 - 5s5d^3D_2$ (497 nm), for a magneto-optical trap (MOT) of Sr atoms. We reveal that the enhancement in the MOT lifetime is limited to 26.9(2) for any single-repumping scheme. Our investigation indicates that the primary decay path from the $5s5p^1P_1$ state to the $5s5p^3P_0$ state proceeds via the $5s4d^3D_1$ state, rather than through the upper states accessed by the single-repumping lasers. We estimate that the branching ratio for the $5s5p^1P_1 \rightarrow 5s4d^3D_1 \rightarrow 5s5p^3P_0$ decay path is $1 : 3.9 \times 10^6$ and the decay rate for the transition from the $5s5p^1P_1$ state to the $5s4d^3D_1$ state is $83(32)\text{s}^{-1}$. This outcome underscores the limitation on atom number in the MOT for long loading times ($\gtrsim 1\text{s}$) when employing a single-repumping scheme. These findings will contribute to the construction of field-deployable optical lattice clocks.

I. INTRODUCTION

The electronic structure of alkaline-earth-metal (-like) atoms is characterized by the presence of long-lived metastable states and ultra-narrow transitions, offering a diverse array of applications such as precision measurements [1–8], tests of special relativity [9], detection of gravitational redshift [10–12], quantum simulation [13], quantum information [14] and search for fundamental physics [15], including gravitational wave detection [16, 17] and search for dark matter [17, 18]. Particularly, optical lattice clocks utilizing Sr have been intensively studied as promising candidates for redefining the second [19].

In a standard magneto-optical trap (MOT) of Sr atoms, the $5s^2^1S_0 - 5s5p^1P_1$ transition (461 nm) is typically employed. However, this transition is not completely closed; the atoms can decay from the $5s5p^1P_1$ state to the $5s4d^1D_2$ state with a branching ratio of $1 : 50\,000$ [20, 21]. Subsequently, atoms in the $5s4d^1D_2$ state further decay to the $5s5p^3P_2$ and $5s5p^3P_1$ states at a ratio of 2:1 [21, 22]. Those atoms decaying to the $5s5p^3P_1$ state return to the $5s^2^1S_0$ state at a rate of $4.7 \times 10^4\text{s}^{-1}$ [23] and are subsequently recaptured in the MOT. Conversely, atoms decaying to the $5s5p^3P_2$ state leak out of the trap because the lifetime of the $5s5p^3P_2$ state is approximately 10^3s [24, 25]. Therefore, an additional laser repumping the atoms in the 3P_2 state to the $5s5p^3P_1$ state is required.

Earlier experiments utilized the $5s5p^3P_2 - 5s6s^3S_1$ (707 nm) transition for repumping the atoms in the $5s5p^3P_2$ state. However, atoms excited to the $5s6s^3S_1$ state can decay to the long-lived $5s5p^3P_0$ state [26, 27], necessitating another laser at the $5s5p^3P_0 - 5s6s^3S_1$ (679 nm) transition [28].

Recently, single-repumping schemes have also been demonstrated, specifically using $5s5p^3P_2 - 5s5d^3D_2$

(497 nm) [29], $5s5p^3P_2 - 5s6d^3D_2$ (403 nm) [30], $5s5p^3P_2 - 5p^2^3P_2$ (481 nm) [31], and $5s5p^3P_2 - 5s4d^3D_2$ (3012 nm) [32]. If the upper state of the repumping transition had a negligible decay rate to the $5s5p^3P_0$ state, the single-repumping scheme would suffice. However, all previous studies utilizing a single-repumping scheme have reported that the trap lifetime ($< 1\text{s}$) was much shorter than the vacuum-limited value ($\sim 10\text{s}$).

For a MOT of Yb atoms using the $6s^2^1S_0 - 6s6p^1P_1$ (399 nm) transition, the dominant loss channel is the decay path of $6s6p^1P_1 \rightarrow 6s5d^3D_1 \rightarrow 6s6p^3P_0$, limiting the trap lifetime to $\sim 1\text{s}$ [33, 34]. However, for a Sr MOT, the decay path of $5s5p^1P_1 \rightarrow 5s4d^3D_1 \rightarrow 5s5p^3P_0$ has rarely been discussed [30]. To our knowledge, there has been no measurement of the branching ratio for the transition from the $5s5p^1P_1$ state (via the $5s4d^3D_1$ state) to the $5s5p^3P_0$ state.

In this study, we investigate the performance of a MOT of ^{88}Sr atoms for two single-repumping schemes: $5s5p^3P_2 - 5p^2^3P_2$ (481 nm) and $5s5p^3P_2 - 5s5d^3D_2$ (497 nm). Our findings reveal that the enhancement in the MOT lifetime is 26.9(2), irrespective of both the single-repumping transition and the trapped atom density. This outcome indicates that the dominant decay path from the $5s5p^1P_1$ state to the $5s5p^3P_0$ state is via the $5s4d^3D_1$ state ($5s5p^1P_1 \rightarrow 5s4d^3D_1 \rightarrow 5s5p^3P_0$). Additionally, we estimate that the branching ratio for the transition from the $5s5p^1P_1$ state (via the $5s4d^3D_1$ state) to the $5s5p^3P_0$ state is $1 : 3.9 \times 10^6$ and the decay rate for the transition from the $5s5p^1P_1$ state to the $5s4d^3D_1$ state is $83(32)\text{s}^{-1}$. These findings underscore that, when a long loading time ($\gtrsim 1\text{s}$) is necessary, the atom number in the MOT is significantly limited for single-repumping schemes. This revelation will aid in the development of field-deployable optical lattice clocks.

II. EXPERIMENTAL SETUP

Figure 1 shows the energy levels and decay rates of Sr relevant to our investigation. The laser for trapping drives the $5s^2^1S_0 - 5s5p^1P_1$ (461 nm) transition. Ad-

* okamoto@ecc.u-tokyo.ac.jp

† ytorii@phys.c.u-tokyo.ac.jp

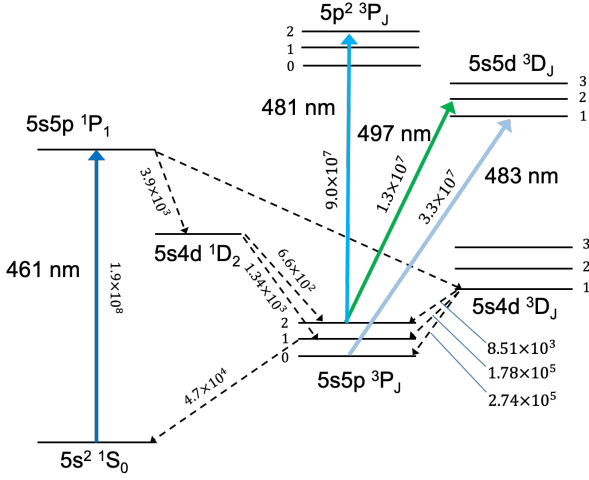


FIG. 1. Relevant energy levels for Sr with transition decay rates (in s^{-1}). Solid arrows indicate transitions utilized in our study whereas dashed lines represent relevant decay paths. See Appendix D for references on decay rates.

ditional lasers are employed to address specific transitions for repumping: the $5s5p^3P_2 - 5p^2^3P_2$ transition at 481 nm, and the $5s5p^3P_2 - 5s5d^3D_2$ transition at 497 nm to compare the two 3P_2 repumping schemes, and the $5s5p^3P_0 - 5s5d^3D_1$ transition at 483 nm for 3P_0 repumping. All the lasers are homemade external-cavity diode lasers (ECDL).

The MOT is composed of three retroreflected beams at 461 nm with a diameter of 18 mm and a combined power of 65 mW yielding a total intensity at the MOT position of 48 mW/cm^2 , estimated from MOT lifetime measurements (see Appendix C). The axial magnetic field gradient of the MOT coils is 50 G/cm. The repumping beams, each with a power of a few mW and a diameter of about 5 mm, have sufficient intensities; halving their power does not degrade the MOT performance. The frequencies of these lasers are stabilized using birefringent atomic vapor laser lock (BAVLL) employing a hollow cathode lamp [35]. The detuning of the trapping light is adjusted by introducing an offset to the BAVLL signal, while the frequencies of all the repumping lasers are locked at resonance.

The details of the vacuum system will be described elsewhere. In summary, a compact oven with capillaries, following a design inspired by Ref. [36], is utilized for loading atoms in the MOT. The atoms are loaded in the MOT directly from a thermal atomic beam derived from the oven as demonstrated for Li [37] and Ca [38]. The atoms are trapped in a glass cell ($25 \text{ mm} \times 25 \text{ mm} \times 100 \text{ mm}$), and the entire vacuum system is evacuated by a single 55-l/s ion pump. The distance between the oven and the MOT region is 37 cm. The oven temperature is set to 335°C , resulting in a MOT loading rate of 5.0×10^5 atoms/s and a vacuum

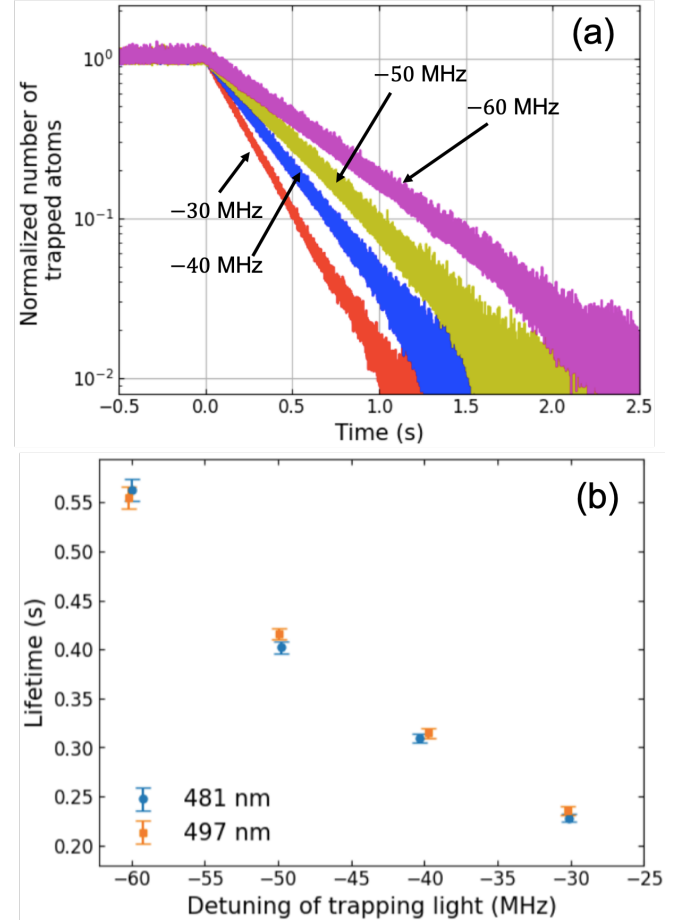


FIG. 2. (a) Normalized number of trapped atoms after turning off the 3P_0 repumping laser (483 nm) while maintaining the 3P_2 repumping laser (481 nm) and varying the trapping light (461 nm) detuning. (b) Variation in lifetime with trapping light detuning for the two 3P_2 repumping lasers operating at 481 nm and 497 nm.

pressure of $\sim 1 \times 10^{-10}$ Torr. Under these conditions, with both the $5s5p^3P_2$ and $5s5p^3P_0$ repumping laser beams on, the number of trapped atoms is $\sim 2 \times 10^6$ as estimated by measuring fluorescence using a photodiode. The observed decay of trapped atoms, after shutting off the atomic beam, exhibits a lifetime of 15 s, which is presumably limited by background gas collisions.

III. RESULTS AND DISCUSSION

To estimate the decay rate for the transition from the $5s5p^1P_1$ state to the $5s5p^3P_0$ state for the two single-repumping schemes, we initially load the MOT using both the 3P_0 (483 nm) and 3P_2 (481 nm or 497 nm) repumping laser beams, followed by turning off the 3P_0 repumping laser beam. Figure 2(a) shows the decay of atom number in the MOT after turning off the 483-nm repumping light at various detunings of the trapping light

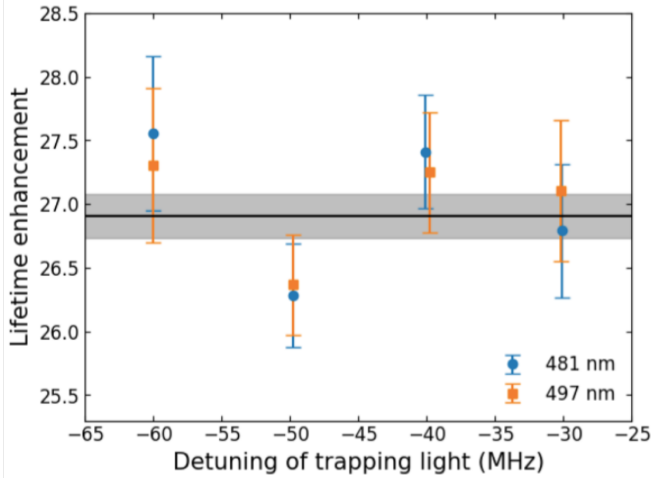


FIG. 3. Enhancement in the lifetimes of the MOT for two single-repumping schemes operating at 481 nm and 497 nm. The solid line is the weighted average of the data. The gray band represents the overall $\pm 1\sigma$ statistical uncertainty. Error bars indicate the uncertainty in fitting the decay data, as depicted in Fig. 2(a). The reduced χ^2 value for the combined data is 1.1, with a P value of 0.3.

(461 nm) when utilizing the 481-nm light. Figure 2(b) shows the dependence of the lifetime on the detuning of the trapping light for both the 481-nm and 497-nm repumping laser beams, indicating that the decay rate for the transition from the $5s5p^1P_1$ state to the $5s5p^3P_0$ state is independent of the choice of the 3P_2 repumping transition. The MOT lifetime increases with larger detuning because the fraction of atoms in the $5s5p^1P_1$ state diminishes with detuning as outlined in Eqs. (A3) and (A9) in Appendix A.

To assess the improvement in lifetime for the two single-repumping schemes, we also measure the decay rate for the transition from the $5s5p^1P_1$ state to the $5s5p^3P_2$ state by turning off the 3P_2 (481 nm or 497 nm) repumping light while maintaining the 3P_0 (483 nm) repumping light (see Appendix A). Figure 3 shows the enhancement, defined as the ratio of the MOT lifetimes with and without the single-repumping light (481 nm or 497 nm) for various detunings. This enhancement remains unaffected by both the single-repumping transition and the detuning of the trapping light. The weighted average enhancement factor is 26.9(2), consistent with the previously reported value of 32(5) for the 497-nm repumping scheme [30]. We note that Fig. 3 indicates the enhancement factor is independent of the density of the trapped atoms because the density significantly depends on the detuning as described in Ref. [21].

The MOT lifetime, depicted in Fig. 2(a), using solely the 3P_2 (481 nm or 497 nm) repumping light, is less than 1 s, considerably shorter compared with when both the 3P_2 and 3P_0 repumping laser beams are employed (15 s). Previous studies employing a single-repumping

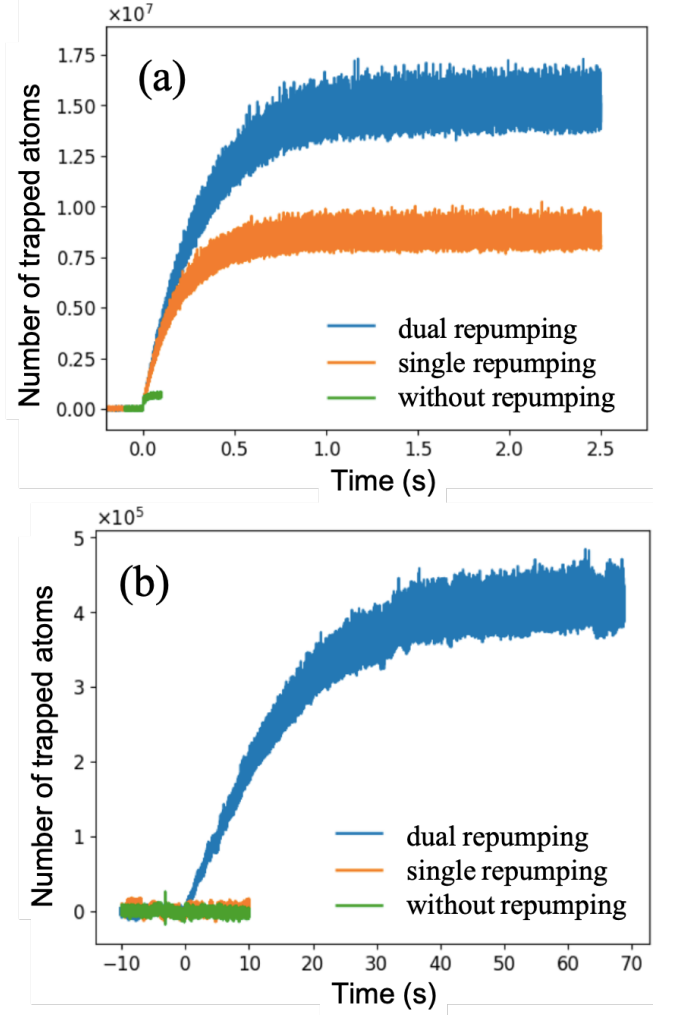


FIG. 4. Evolution of the trapped atom number after turning on the MOT coils at oven temperatures of (a) 455 °C and (b) 285 °C under various repumping conditions: no repumping, single repumping operating at 481 nm, and dual repumping operating at 481 nm and 483 nm. The detuning of the trapping light is -40 MHz.

scheme also consistently reported trap lifetimes of less than 1 s [30–32, 39]. The decay from the upper state of the repumping transition to the 3P_0 state via intermediate states was mentioned [30, 31, 39–41]. If this hypothesis is the case, the enhancement factor should depend on the upper state (see Appendix A). However, as depicted in Fig. 3, the enhancement factor remains unaffected by both the two single-repumping schemes, indicating that the decay from the upper state of the repumping transition to the 3P_0 state is negligible. This is supported by the fact that, for the 497 nm repumping scheme, the branching ratio for the dipole-allowed transitions [$5s5d^3D_2 \rightarrow 5s6p^3P_2 \rightarrow 5s6s^3S_1 (5s4d^3D_1) \rightarrow 5s5d^3P_0$] was estimated to be quite small (0.035%) [30], and, for the 481 nm repumping scheme, there is no inter-

mediate states through which the upper state $5p^2\ ^3P_2$ is connected to the $5s5p\ ^3P_0$ state by dipole-allowed transitions [42].

As an alternative reason for the shorter MOT lifetimes for single-repumping schemes, binary collisional loss involving atoms in excited states was also mentioned [31]. However, the single exponential decay observed in trapped atoms, as depicted in Fig. 2(a), rules out possible decay due to binary collisions. This is further supported by Fig. 3, showing that the MOT lifetime enhancement is unaffected by detuning of the trapping light (i.e., MOT density).

Our results strongly indicate, as discussed in Appendix B, that the primary decay path from the $5s5p\ ^1P_1$ state to the $5s5p\ ^3P_0$ state proceeds via the $5s4d\ ^3D_1$ state as shown in Fig. 1 ($5s5p\ ^1P_1 \rightarrow 5s4d\ ^3D_1 \rightarrow 5s5p\ ^3P_0$). The branching ratio from the $5s5p\ ^1P_1$ state (via the $5s4d\ ^3D_1$ state) to the $5s5p\ ^3P_0$ state is $1 : 3.9 \times 10^6$, derived from the branching ratio for the transition from the $5s5p\ ^1P_1$ state (via the $5s4d\ ^1D_2$ state) to the $5s5p\ ^3P_2$ state ($1 : 150\,000$) [20–22] and the observed enhancement factor of 26.9(2). Considering the branching ratio for the transition from the $5s4d\ ^3D_1$ state to the $5s5p\ ^3P_1$ state (60%) [43], the decay rate for the transition from the $5s5p\ ^1P_1$ state to the $5s4d\ ^3D_1$ state is $83(32)\text{ s}^{-1}$ (see Appendix B); the uncertainty primarily arises from the decay rate for the transition from the $5s5p\ ^1P_1$ state to the $5s4d\ ^1D_2$ state [$3.9(1.5) \times 10^3\text{ s}^{-1}$] [20].

Our results indicate that for a single-repumping scheme, if the loading rate of atoms is low enough to require a long loading time ($\gtrsim 1\text{ s}$), the atom number in the MOT is considerably limited. This is experimentally demonstrated in Fig. 4. For instance, at an oven temperature of 455°C with a loading rate of $4 \times 10^7\text{ s}^{-1}$, the number of trapped atoms saturates within 1 s and the reduction in the number of trapped atoms for the single-repumping scheme is only 40% compared with the dual-repumping scheme [Fig. 4(a)]. Conversely, at an oven temperature of 285°C with a loading rate of $2 \times 10^4\text{ s}^{-1}$, the loading time of the MOT for the dual-repumping scheme exceeds 10 s, and the number of trapped atoms is less than 10^4 for the single-repumping scheme, being only 1/50 of that for the dual-repumping scheme [Fig. 4(b)].

Considering the requirements for field-deployable or spaceborne optical lattice clocks [10, 44–50], a small-sized and energy-saving atomic beam source is essential. Achieving these goals necessitates operating the atom oven at low temperatures and avoiding the use of Zeeman slower and 2-dimensional MOTs [51, 52]. In this scenario, from which high MOT loading rates cannot be expected, a dual-repumping scheme should be adopted.

IV. CONCLUSION

We conducted a comparative analysis of a MOT of ^{88}Sr atoms for two single-repumping schemes (481 nm and 497 nm). Our investigation revealed that the enhance-

ment in lifetime was consistent at 26.9(2), demonstrating independence not only from the single-repumping transition but also from the density of trapped atoms. This outcome indicates that the primary decay path from the $5s5p\ ^1P_1$ state to the $5s5p\ ^3P_0$ state proceeds via the $5s4d\ ^3D_1$ state ($5s5p\ ^1P_1 \rightarrow 5s4d\ ^3D_1 \rightarrow 5s5p\ ^3P_0$), a mechanism previously overlooked. Owing to this decay path, the trapped atom number should be significantly restricted when employing a single-repumping scheme, particularly when a long loading time ($\gtrsim 1\text{ s}$) is required. We estimated the branching ratio for the transition from the $5s5p\ ^1P_1$ state (via the $5s4d\ ^3D_1$ state) to the $5s5p\ ^3P_0$ state to be $1 : 3.9 \times 10^6$ and the decay rate for the transition from the $5s5p\ ^1P_1$ state to the $5s4d\ ^3D_1$ state to be $83(32)\text{ s}^{-1}$. Our findings underscore the need to reevaluate single-repumping schemes for Sr laser cooling.

V. ACKNOWLEDGMENTS

We thank T. Sato and M. Mori for their contributions to the experiments. This work was supported by JSPS KAKENHI Grant Numbers 23K20849 and 22KJ1163.

Appendix A: Rate equations

We present the rate equations describing the number of trapped atoms for various schemes:

1. dual-repumping (3P_2 and 3P_0) scheme
2. scheme with only the 3P_0 repumping laser
3. single-repumping (3P_2) scheme
4. scheme with no repumping laser

For scheme 1, the rate equation for the number of trapped atoms is given by

$$\frac{dN}{dt} = R - \gamma_c N - \beta N^2, \quad (\text{A1})$$

where N denotes the number of trapped atoms, R the atom loading rate, γ_c the background collisional loss rate, and β the coefficient for two-body collisional loss. Under our experimental conditions (oven temperature of 335°C), γ_c and βN are of the order of 0.1 s^{-1} , confirmed by observing the decay of the number of trapped atoms after shutting off the atomic beam.

For scheme 2, in which atoms decaying to the 3P_2 state are lost, the rate equation is given by

$$\frac{dN}{dt} = R - f a_2 N - \gamma_c N - \beta N^2, \quad (\text{A2})$$

where a_2 denotes the decay rate for the transition from the 1P_1 state to the 3P_2 state and f the excitation fraction of the $5s^2\ ^1S_0 - 5s5p\ ^1P_1$ (461 nm) transition, which

is given by

$$f = \frac{1}{2} \frac{s_0}{1 + s_0 + 4(\Delta/\Gamma)^2}, \quad (\text{A3})$$

where $s_0 = I/I_s$ (I being the 461-nm laser beam intensity and $I_s = 40 \text{ mW/cm}^2$ the saturation intensity) denotes the resonant saturation parameter, Δ the detuning, and $\Gamma = 2\pi \times 30 \text{ MHz}$ the natural width. According to Ref. [21], a_2 is given by

$$a_2 = A_{1P_1 \rightarrow 1D_2} B_{1D_2 \rightarrow 3P_2}, \quad (\text{A4})$$

where $A_{1P_1 \rightarrow 1D_2} = 3.85(1.47) \times 10^3 \text{ s}^{-1}$ [20] denotes the decay rate for the transition from the $1P_1$ state to the $1D_2$ state, and $B_{1D_2 \rightarrow 3P_2} = 0.33$ [22] the branching ratio from the $1D_2$ state to the $3P_2$ state. Because the value of f is typically ~ 0.1 for a standard MOT, fa_2 is $\sim 100 \text{ s}^{-1}$, which is much larger than γ_c and βN . Thus, Eq. (A2) can be approximated by

$$\frac{dN}{dt} = R - fa_2N = R - \frac{N}{\tau_2}, \quad (\text{A5})$$

where τ_2 is the lifetime of the MOT only with $3P_0$ repumping laser, which is expressed as

$$\tau_2 = \frac{1}{fA_{1P_1 \rightarrow 1D_2} B_{1D_2 \rightarrow 3P_2}}. \quad (\text{A6})$$

For scheme 3, in which atoms decaying to the $3P_0$ state are lost, the rate equation is given by

$$\frac{dN}{dt} = R - fa_0(X)N - \gamma_c N - \beta N^2, \quad (\text{A7})$$

where $a_0(X)$ denotes the decay rate for the transition from the $1P_1$ state to the $3P_0$ state, and X the upper state of the single-repumping transition ($X = 5p^2 3P_2$ for 481 nm and $X = 5s5d^3 D_2$ for 497 nm). From Fig. 2(a), the observed decay rates of the MOT for the single-repumping scheme are of order 10 s^{-1} , which is still much larger than γ_c and βN . Therefore, Eq. (A7) can be approximated by

$$\frac{dN}{dt} = R - fa_0(X)N = R - \frac{N}{\tau_0(X)}, \quad (\text{A8})$$

where $\tau_0(X)$ is the MOT lifetime, which is expressed as

$$\tau_0(X) = \frac{1}{fa_0(X)}. \quad (\text{A9})$$

For scheme 4, in which atoms decaying to the $3P_0$ or $3P_2$ state are lost, the rate equation is given by

$$\frac{dN}{dt} = R - f(a_0(X) + a_2)N = R - \frac{N}{\tau_{\text{norep}}(X)}, \quad (\text{A10})$$

for which terms $\gamma_c N$ and βN^2 are neglected, as in the scheme above, and $\tau_{\text{norep}}(X)$ denotes the MOT lifetime, expressed as

$$\tau_{\text{norep}}(X) = \frac{1}{f(a_0(X) + a_2)}. \quad (\text{A11})$$

To eliminate the uncertainty in the estimation of f , we measure the ratio $r(X) = \tau_0(X)/\tau_2$, which is expressed as

$$r(X) = \frac{a_2}{a_0(X)}. \quad (\text{A12})$$

The enhancement factor $\epsilon(X) = \tau_0(X)/\tau_{\text{norep}}$ for the single-repumping scheme is then given by

$$\epsilon(X) = \frac{a_0(X) + a_2}{a_0(X)} = 1 + r(X). \quad (\text{A13})$$

Appendix B: Estimation of the decay rate from the $5s5p^1 P_1$ state to the $5s4d^3 D_1$ state

The energy levels of the $5s4d^1 D_2$ state and the $5s4d^3 D_J$ state are below the $5s5p^1 P_1$ state (see Fig. 1). However, there is no electric-dipole allowed (E1) decay path from the $5s5p^1 P_1$ state to the $5s5p^3 P_0$ state through these states. Our experimental results show the decay from the upper state of the $5s5p^3 P_2$ repumping transition to the $3P_0$ state via intermediate states is negligible. Therefore, we need to identify the decay path from the $5s5p^1 P_1$ state to the $5s5p^3 P_0$ state via the $5s4d^1 D_2$ state or the $5s4d^3 D_J$ state. Considering that the decay rate for the spin-forbidden transition of $5s4d^1 D_2 - 5s5p^3 P_2$ ($1.9 \mu\text{m}$) is 661.1 s^{-1} (see Table I in Appendix D), it is reasonable to expect that the decay rates for the spin-forbidden transition of $5s5p^1 P_1 - 5s4d^3 D_1$ ($2.8 \mu\text{m}$) is of order $10^2 \sim 10^3 \text{ s}^{-1}$. Thus, we assume that the primary decay path from the $5s5p^1 P_1$ state to the $5s5p^3 P_0$ state is $5s5p^1 P_1 \rightarrow 5s4d^3 D_1 \rightarrow 5s5p^3 P_0$.

Under this assumption, a_0 can be expressed as

$$a_0 = A_{1P_1 \rightarrow 3D_1} B_{3D_1 \rightarrow 3P_0}, \quad (\text{B1})$$

where $A_{1P_1 \rightarrow 3D_1}$ denotes the decay rate for the transition from the $1P_1$ state to the $3D_1$ state, and $B_{3D_1 \rightarrow 3P_0} = 0.595$ [43] the branching ratio from the $3D_1$ state to the $3P_0$ state. From Eqs. (A12) and (B1), $A_{1P_1 \rightarrow 3D_1}$ is expressed as

$$A_{1P_1 \rightarrow 3D_1} = \frac{a_2}{r B_{3D_1 \rightarrow 3P_0}} = \frac{A_{1P_1 \rightarrow 1D_2} B_{1D_2 \rightarrow 3P_2}}{r B_{3D_1 \rightarrow 3P_0}}. \quad (\text{B2})$$

All the constants on the right-hand side of Eq. (B2) are known from the previous studies and our experiments: $A_{1P_1 \rightarrow 1D_2} = 3.85(1.47) \times 10^3 \text{ s}^{-1}$ [20], $B_{1D_2 \rightarrow 3P_2} = 0.33$ [22], $B_{3D_1 \rightarrow 3P_0} = 0.595$ [43], $r = \epsilon - 1 = 25.9(2)$ [see Eq. (A13) and Fig. 3]. Then, one can calculate the decay rate for the $5s5p^1 P_1 - 5s4d^3 D_1$ transition as $A_{1P_1 \rightarrow 3D_1} = 83(32) \text{ s}^{-1}$.

Appendix C: Estimation of the excitation fraction and the saturation parameter

In general, estimating the total intensity of the MOT beam by measuring the beam power is difficult because of

the uncertainties in gauging the shape of the beam and the loss of beam power in various optical components. To circumvent this problem, we adopt a method based on the excitation fraction.

From Eq. (A6), the excitation fraction of the 461-nm transition is expressed as

$$f = \frac{1}{\tau_2 A_{1P_1 \rightarrow 1D_2} B_{1D_2 \rightarrow 3P_2}}, \quad (\text{C1})$$

where τ_2 denotes the MOT lifetime obtained only with a 3P_0 repumping laser; the values of $A_{1P_1 \rightarrow 1D_2}$ and $B_{1D_2 \rightarrow 3P_2}$ are found in Ref. [20] and [22], respectively (see Appendix D). Using Eq. (C1), we can estimate f by measuring τ_2 with a relative uncertainty of 40%, stemming mainly from that of $A_{1P_1 \rightarrow 1D_2}$. From Eq. (A3), we can infer the resonant saturation parameter s_0 , and hence the total intensity $I = s_0 I_s$, where $I_s = 40 \text{ mW/cm}^2$ is the saturation intensity.

Appendix D: List of the decay rates

We list the decay rates for the transitions relevant to our work in Table. I.

TABLE I. Decay rates for transitions relevant to the present work.

Transition	Decay rate (s^{-1})	Ref.
$5s^2 1S_0 - 5s5p^1P_1$	$1.900(1) \times 10^8$	[53]
$5s^2 1S_0 - 5s5p^3P_1$	$4.7(1) \times 10^4$	[23]
$5s5p^1P_1 - 5s4d^1D_2$	$3.85(1.47) \times 10^3$	[20]
$5s4d^1D_2 - 5s5p^3P_2$	661.1	[22]
$5s4d^1D_2 - 5s5p^3P_1$	1344.0	[22]
$5s4d^3D_1 - 5s5p^3P_2$	8.510×10^3	[43]
$5s4d^3D_1 - 5s5p^3P_1$	1.777×10^5	[43]
$5s4d^3D_1 - 5s5p^3P_0$	2.740×10^5	[43]
$5s5p^3P_2 - 5p^2 3P_2$	$9.0(6) \times 10^7$	[42]
$5s5p^3P_2 - 5s5d^3D_2$	$1.28(9) \times 10^7$	[42]
$5s5p^3P_0 - 5s5d^3D_1$	$3.3(2) \times 10^7$	[42]

-
- [1] S. L. Campbell, R. B. Hutson, G. E. Marti, A. Goban, N. D. Oppong, R. L. McNally, L. Sonderhouse, J. M. Robinson, W. Zhang, B. J. Bloom, and J. Ye, A fermi-degenerate three-dimensional optical lattice clock, *Science* **358**, 90 (2017).
- [2] E. Oelker, R. B. Hutson, C. J. Kennedy, L. Sonderhouse, T. Bothwell, A. Goban, D. Kedar, C. Sanner, J. M. Robinson, G. E. Marti, D. G. Matei, T. Legero, M. Giunta, R. Holzwarth, F. Riehle, U. Sterr, and J. Ye, Demonstration of 4.8×10^{-17} stability at 1 s for two independent optical clocks, *Nature Photonics* **13**, 714 (2019).
- [3] T. L. Nicholson, S. L. Campbell, R. B. Hutson, G. E. Marti, B. J. Bloom, R. L. McNally, W. Zhang, M. D. Barrett, M. S. Safronova, G. F. Strouse, W. L. Tew, and J. Ye, Systematic evaluation of an atomic clock at 2×10^{-18} total uncertainty, *Nature Communications* **6**, 6896 (2015).
- [4] W. F. McGrew, X. Zhang, R. J. Fasano, S. A. Schäffer, K. Beloy, D. Nicolodi, R. C. Brown, N. Hinkley, G. Milani, M. Schioppa, T. H. Yoon, and A. D. Ludlow, Atomic clock performance enabling geodesy below the centimetre level, *Nature* **564**, 87 (2018).
- [5] S. M. Brewer, J.-S. Chen, A. M. Hankin, E. R. Clements, C. W. Chou, D. J. Wineland, D. B. Hume, and D. R. Leibbrandt, $^{27}\text{Al}^+$ quantum-logic clock with a systematic uncertainty below 10^{-18} , *Phys. Rev. Lett.* **123**, 033201 (2019).
- [6] T. Bothwell, D. Kedar, E. Oelker, J. M. Robinson, S. L. Bromley, W. L. Tew, J. Ye, and C. J. Kennedy, Jila sri optical lattice clock with uncertainty of 2.0×10^{-18} , *Metrologia* **56**, 065004 (2019).
- [7] N. Nemitz, T. Ohkubo, M. Takamoto, I. Ushijima, M. Das, N. Ohmae, and H. Katori, Frequency ratio of yb and sr clocks with 5×10^{-17} uncertainty at 150 seconds averaging time, *Nature Photonics* **10**, 258 (2016).
- [8] K. Beloy, M. I. Bodine, T. Bothwell, S. M. Brewer, S. L. Bromley, J.-S. Chen, J.-D. Deschênes, S. A. Diddams, R. J. Fasano, T. M. Fortier, Y. S. Hassan, D. B. Hume, D. Kedar, C. J. Kennedy, I. Khader, A. Koepke, D. R. Leibbrandt, H. Leopardi, A. D. Ludlow, W. F. McGrew, W. R. Milner, N. R. Newbury, D. Nicolodi, E. Oelker, T. E. Parker, J. M. Robinson, S. Romisch, S. A. Schäffer, J. A. Sherman, L. C. Sinclair, L. Sonderhouse, W. C. Swann, J. Yao, J. Ye, X. Zhang, and B. A. C. O. N. B. Collaboration*, Frequency ratio measurements at 18-digit accuracy using an optical clock network, *Nature* **591**, 564 (2021).
- [9] P. Delva, J. Lodewyck, S. Bilicki, E. Bookjans, G. Vallet, R. Le Targat, P.-E. Pottie, C. Guerlin, F. Meynadier, C. Le Poncin-Lafitte, O. Lopez, A. Amy-Klein, W.-K. Lee, N. Quintin, C. Lisdar, A. Al-Masoudi, S. Dörscher, C. Grebing, G. Grosche, A. Kuhl, S. Raupach, U. Sterr, I. R. Hill, R. Hobson, W. Bowden, J. Kronjäger, G. Marra, A. Rolland, F. N. Baynes, H. S. Margolis, and P. Gill, Test of special relativity using a fiber network of optical clocks, *Phys. Rev. Lett.* **118**, 221102 (2017).
- [10] M. Takamoto, I. Ushijima, N. Ohmae, T. Yahagi, K. Kokado, H. Shinkai, and H. Katori, Test of general relativity by a pair of transportable optical lattice clocks, *Nature Photonics* **14**, 411 (2020).
- [11] T. Bothwell, C. J. Kennedy, A. Aeppli, D. Kedar, J. M. Robinson, E. Oelker, A. Staron, and J. Ye, Resolving the gravitational redshift across a millimetre-scale atomic sample, *Nature* **602**, 420 (2022).
- [12] X. Zheng, J. Dolde, M. C. Cambria, H. M. Lim, and S. Kolkowitz, A lab-based test of the gravitational redshift with a miniature clock network, *Nature Communications* **14**, 4886 (2023).
- [13] S. Kolkowitz, S. L. Bromley, T. Bothwell, M. L. Wall, G. E. Marti, A. P. Koller, X. Zhang, A. M. Rey, and J. Ye, Spin-orbit-coupled fermions in an optical lattice clock, *Nature* **542**, 66 (2017).

- [14] M. A. Norcia, A. W. Young, W. J. Eckner, E. Oelker, J. Ye, and A. M. Kaufman, Seconds-scale coherence on an optical clock transition in a tweezer array, *Science* **366**, 93 (2019).
- [15] M. S. Safronova, D. Budker, D. DeMille, D. F. J. Kimball, A. Derevianko, and C. W. Clark, Search for new physics with atoms and molecules, *Rev. Mod. Phys.* **90**, 025008 (2018).
- [16] S. Kolkowitz, I. Pikovski, N. Langellier, M. D. Lukin, R. L. Walsworth, and J. Ye, Gravitational wave detection with optical lattice atomic clocks, *Phys. Rev. D* **94**, 124043 (2016).
- [17] M. Abe, P. Adamson, M. Borcean, D. Bortoletto, K. Bridges, S. P. Carman, S. Chattopadhyay, J. Coleman, N. M. Curfman, K. DeRose, T. Deshpande, S. Dimopoulos, C. J. Foot, J. C. Frisch, B. E. Garber, S. Geer, V. Gibson, J. Glick, P. W. Graham, S. R. Hahn, R. Harnik, L. Hawkins, S. Hindley, J. M. Hogan, Y. Jiang, M. A. Kasevich, R. J. Kellett, M. Kiburg, T. Kovachy, J. D. Lykken, J. March-Russell, J. Mitchell, M. Murphy, M. Nantel, L. E. Nobrega, R. K. Plunkett, S. Rajendran, J. Rudolph, N. Sachdeva, M. Safdari, J. K. Santucci, A. G. Schwartzman, I. Shipsey, H. Swan, L. R. Valerio, A. Vasonis, Y. Wang, and T. Wilkason, Matter-wave atomic gradiometer interferometric sensor (magis-100), *Quantum Science and Technology* **6**, 044003 (2021).
- [18] T. Kobayashi, A. Takamizawa, D. Akamatsu, A. Kawasaki, A. Nishiyama, K. Hosaka, Y. Hisai, M. Wada, H. Inaba, T. Tanabe, and M. Yasuda, Search for ultralight dark matter from long-term frequency comparisons of optical and microwave atomic clocks, *Phys. Rev. Lett.* **129**, 241301 (2022).
- [19] N. Dimarcq, M. Gertszov, G. Mileti, S. Bize, C. W. Oates, E. Peik, D. Calonico, T. Ido, P. Tavella, F. Meynadier, G. Petit, G. Panfilo, J. Bartholomew, P. De-fraigne, E. A. Donley, P. O. Hedekvist, I. Sesia, M. Wouters, P. Dubé, F. Fang, F. Levi, J. Lodewyck, H. S. Margolis, D. Newell, S. Slyusarev, S. Weyers, J.-P. Uzan, M. Yasuda, D.-H. Yu, C. Rieck, H. Schnatz, Y. Hanado, M. Fujieda, P.-E. Pottie, J. Hanssen, A. Malimon, and N. Ashby, Roadmap towards the redefinition of the second, *Metrologia* **61**, 012001 (2024).
- [20] L. R. Hunter, W. A. Walker, and D. S. Weiss, Observation of an atomic stark-electric-quadrupole interference, *Phys. Rev. Lett.* **56**, 823 (1986).
- [21] X. Xu, T. H. Loftus, J. L. Hall, A. Gallagher, and J. Ye, Cooling and trapping of atomic strontium, *J. Opt. Soc. Am. B* **20**, 968 (2003).
- [22] C. W. B. Jr, S. R. Langhoff, and H. Partridge, The radiative lifetime of the 1d2 state of ca and sr: a core-valence treatment, *Journal of Physics B: Atomic and Molecular Physics* **18**, 1523 (1985).
- [23] R. Drozdowski, M. Ignaciuk, J. Kwela, and J. Heldt, Radiative lifetimes of the lowest 3p1 metastable states of ca and sr, *Zeitschrift für Physik D Atoms, Molecules and Clusters* **41**, 125 (1997).
- [24] A. Derevianko, Feasibility of cooling and trapping metastable alkaline-earth atoms, *Phys. Rev. Lett.* **87**, 023002 (2001).
- [25] M. Yasuda and H. Katori, Lifetime measurement of the 3p_2 metastable state of strontium atoms, *Phys. Rev. Lett.* **92**, 153004 (2004).
- [26] A. V. Taichenachev, V. I. Yudin, C. W. Oates, C. W. Hoyt, Z. W. Barber, and L. Hollberg, Magnetic field-induced spectroscopy of forbidden optical transitions with application to lattice-based optical atomic clocks, *Phys. Rev. Lett.* **96**, 083001 (2006).
- [27] Z. W. Barber, C. W. Hoyt, C. W. Oates, L. Hollberg, A. V. Taichenachev, and V. I. Yudin, Direct excitation of the forbidden clock transition in neutral ^{174}Yb atoms confined to an optical lattice, *Phys. Rev. Lett.* **96**, 083002 (2006).
- [28] K. Vogel, *Laser cooling on a narrow atomic transition and measurement of the two body collision loss rate in a strontium magneto-optical trap*, Ph.D. thesis, University of Colorado (2002).
- [29] N. Poli, R. E. Drullinger, G. Ferrari, J. Léonard, F. Sorrentino, and G. M. Tino, Cooling and trapping of ultracold strontium isotopic mixtures, *Phys. Rev. A* **71**, 061403 (2005).
- [30] S. Stellmer and F. Schreck, Reservoir spectroscopy of $5s5p\ ^3p_2$ - $5snd\ ^3D_{1,2,3}$ transitions in strontium, *Phys. Rev. A* **90**, 022512 (2014).
- [31] F. Hu, I. Nosske, L. Couturier, C. Tan, C. Qiao, P. Chen, Y. H. Jiang, B. Zhu, and M. Weidemüller, Analyzing a single-laser repumping scheme for efficient loading of a strontium magneto-optical trap, *Phys. Rev. A* **99**, 033422 (2019).
- [32] P. G. Mickelson, Y. N. M. de Escobar, P. Anzel, B. J. DeSalvo, S. B. Nagel, A. J. Traverso, M. Yan, and T. C. Killian, Repumping and spectroscopy of laser-cooled sr atoms using the $(5s5p)3p_2$ - $(5s4d)3d_2$ transition, *Journal of Physics B: Atomic, Molecular and Optical Physics* **42**, 235001 (2009).
- [33] S. G. Porsev, Y. G. Rakhlin, and M. G. Kozlov, Electric-dipole amplitudes, lifetimes, and polarizabilities of the low-lying levels of atomic ytterbium, *Phys. Rev. A* **60**, 2781 (1999).
- [34] J. W. Cho, H.-g. Lee, S. Lee, J. Ahn, W.-K. Lee, D.-H. Yu, S. K. Lee, and C. Y. Park, Optical repumping of triplet- p states enhances magneto-optical trapping of ytterbium atoms, *Phys. Rev. A* **85**, 035401 (2012).
- [35] T. Sato, Y. Hayakawa, N. Okamoto, Y. Shimomura, T. Aoki, and Y. Torii, Birefringent atomic vapor laser lock in a hollow cathode lamp, *J. Opt. Soc. Am. B* **39**, 155 (2022).
- [36] M. Schioppo, N. Poli, M. Prevedelli, S. Falke, C. Lisdat, U. Sterr, and G. M. Tino, A compact and efficient strontium oven for laser-cooling experiments, *Review of Scientific Instruments* **83**, 103101 (2012).
- [37] B. P. Anderson and M. A. Kasevich, Enhanced loading of a magneto-optic trap from an atomic beam, *Phys. Rev. A* **50**, R3581 (1994).
- [38] C. W. Oates, F. Bondu, R. W. Fox, and L. Hollberg, A diode-laser optical frequency standard based on laser-cooled ca atoms: Sub-kilohertz spectroscopy by optical shelving detection, *The European Physical Journal D - Atomic, Molecular, Optical and Plasma Physics* **7**, 449 (1999).
- [39] P. H. Moriya, M. O. Araújo, F. Todão, M. Hemmerling, H. Keßler, R. F. Shiozaki, R. C. Teixeira, and P. W. Courteille, Comparison between 403 nm and 497 nm repumping schemes for strontium magneto-optical traps, *Journal of Physics Communications* **2**, 125008 (2018).
- [40] C. Vishwakarma, K. Patel, J. Mangaonkar, J. L. MacLennan, K. Biswas, and U. D. Rapol, Study of loss dynamics of strontium in a magneto-optical trap (2019).

- [41] T. Akatsuka, K. Hashiguchi, T. Takahashi, N. Ohmae, M. Takamoto, and H. Katori, Three-stage laser cooling of sr atoms using the $5s5p^3p_2$ metastable state below doppler temperatures, *Phys. Rev. A* **103**, 023331 (2021).
- [42] J. E. Sansonetti and G. Nave, Wavelengths, Transition Probabilities, and Energy Levels for the Spectrum of Neutral Strontium (SrI), *Journal of Physical and Chemical Reference Data* **39**, 033103 (2010).
- [43] M. S. Safronova, S. G. Porsev, U. I. Safronova, M. G. Kozlov, and C. W. Clark, Blackbody-radiation shift in the sr optical atomic clock, *Phys. Rev. A* **87**, 012509 (2013).
- [44] S. B. Koller, J. Grotti, S. Vogt, A. Al-Masoudi, S. Dörscher, S. Häfner, U. Sterr, and C. Lisdat, Transportable optical lattice clock with 7×10^{-17} uncertainty, *Phys. Rev. Lett.* **118**, 073601 (2017).
- [45] J. Grotti, S. Koller, S. Vogt, S. Häfner, U. Sterr, C. Lisdat, H. Denker, C. Voigt, L. Timmen, A. Rolland, F. N. Baynes, H. S. Margolis, M. Zampaolo, P. Thoumany, M. Pizzocaro, B. Rauf, F. Bregolin, A. Tampellini, P. Barbieri, M. Zucco, G. A. Costanzo, C. Clivati, F. Levi, and D. Calonico, Geodesy and metrology with a transportable optical clock, *Nature Physics* **14**, 437 (2018).
- [46] S. Origlia, M. S. Pramod, S. Schiller, Y. Singh, K. Bongs, R. Schwarz, A. Al-Masoudi, S. Dörscher, S. Herbers, S. Häfner, U. Sterr, and C. Lisdat, Towards an optical clock for space: Compact, high-performance optical lattice clock based on bosonic atoms, *Phys. Rev. A* **98**, 053443 (2018).
- [47] W. Bowden, R. Hobson, I. R. Hill, A. Vianello, M. Schioppo, A. Silva, H. S. Margolis, P. E. G. Baird, and P. Gill, A pyramid mot with integrated optical cavities as a cold atom platform for an optical lattice clock, *Scientific Reports* **9**, 11704 (2019).
- [48] A. Sitaram, P. K. Elgee, G. K. Campbell, N. N. Klimov, S. Eckel, and D. S. Barker, Confinement of an alkaline-earth element in a grating magneto-optical trap, *Review of Scientific Instruments* **91**, 103202 (2020).
- [49] N. Ohmae, M. Takamoto, Y. Takahashi, M. Kokubun, K. Araki, A. Hinton, I. Ushijima, T. Muramatsu, T. Furumiya, Y. Sakai, N. Moriya, N. Kamiya, K. Fujii, R. Muramatsu, T. Shiimado, and H. Katori, Transportable strontium optical lattice clocks operated outside laboratory at the level of 10^{-18} uncertainty, *Advanced Quantum Technologies* **4**, 2100015 (2021).
- [50] Y. B. Kale, A. Singh, M. Gellesch, J. M. Jones, D. Morris, M. Aldous, K. Bongs, and Y. Singh, Field deployable atomics package for an optical lattice clock, *Quantum Science and Technology* **7**, 045004 (2022).
- [51] I. Nosske, L. Couturier, F. Hu, C. Tan, C. Qiao, J. Blume, Y. H. Jiang, P. Chen, and M. Weidemüller, Two-dimensional magneto-optical trap as a source for cold strontium atoms, *Phys. Rev. A* **96**, 053415 (2017).
- [52] M. Barbiero, M. G. Tarallo, D. Calonico, F. Levi, G. Lamporesi, and G. Ferrari, Sideband-enhanced cold atomic source for optical clocks, *Phys. Rev. Appl.* **13**, 014013 (2020).
- [53] M. Yasuda, T. Kishimoto, M. Takamoto, and H. Katori, Photoassociation spectroscopy of ^{88}Sr : Reconstruction of the wave function near the last node, *Phys. Rev. A* **73**, 011403 (2006).